JCB Article

Impaired skin wound healing in peroxisome proliferator–activated receptor (PPAR)α and PPARβ mutant mice

Liliane Michalik,[1] Béatrice Desvergne,[1] Nguan Soon Tan,[1] Sharmila Basu-Modak,[1] Pascal Escher,[1] Jennifer Rieusset,[1] Jeffrey M. Peters,[3] Gürkan Kaya,[2] Frank J. Gonzalez,[3] Jozsef Zakany,[4] Daniel Metzger,[5] Pierre Chambon,[5] Denis Duboule,[4] and Walter Wahli[1]

[1]Institut de Biologie Animale, Université de Lausanne, Bâtiment de Biologie, CH-1015 Lausanne, Switzerland
[2]Department of Dermatology, University Hospital of Geneva, CH-1212 Geneva, Switzerland
[3]Laboratory of Molecular Carcinogenesis, National Cancer Institute, National Institute of Health, Bethesda, MD 20892
[4]Département de Zoologie, Université de Genève, Sciences III, CH-1211 Geneva 4, Switzerland
[5]Institut de Génétique et de Biologie Moléculaire et Cellulaire, Centre National de la Recherche Scientifique/Institut National de la Santé et de la Recherche Médicale/ULP/Collège de France, 67404 Illkirch Cedex, CU de Strasbourg, France

We show here that the α, β, and γ isotypes of peroxisome proliferator–activated receptor (PPAR) are expressed in the mouse epidermis during fetal development and that they disappear progressively from the interfollicular epithelium after birth. Interestingly, PPARα and β expression is reactivated in the adult epidermis after various stimuli, resulting in keratinocyte proliferation and differentiation such as tetradecanoylphorbol acetate topical application, hair plucking, or skin wound healing. Using PPARα, β, and γ mutant mice, we demonstrate that PPARα and β are important for the rapid epithelialization of a skin wound and that each of them plays a specific role in this process. PPARα is mainly involved in the early inflammation phase of the healing, whereas PPARβ is implicated in the control of keratinocyte proliferation. In addition and very interestingly, PPARβ mutant primary keratinocytes show impaired adhesion and migration properties. Thus, the findings presented here reveal unpredicted roles for PPARα and β in adult mouse epidermal repair.

Introduction

The major function of the outermost layer of the skin, the epidermis, is to provide a defense against microbial, mechanical, chemical, and UV light aggressions and to protect the organism from dehydration. The epidermis consists of several layers of keratinocytes which undergo a vectorial differentiation program as they migrate from the basal undifferentiated layer to the outermost layer, the stratum corneum, in which the protective cutaneous function mainly resides (Downing, 1992; Bickenbach et al., 1995; Roop, 1995). The maturation of the epidermis, and thus the formation of a competent barrier against aggressions and water loss, happens in the latest stages of fetal development to be completed before birth (Elias, 1983; Elias and Menon, 1991; Schurer and Elias, 1991). After birth, disruption of the mature skin will leave an opened door to infection and dehydration, a major problem for heavily injured victims. In these cases, the covering of the wound by a new epithelium, termed reepithelialization, starts within hours of the injury and will eventually reconstitute a fully differentiated epithelium that is crucial for the rebuilding of a competent protective epidermis. The reepithelialization of a wound initially involves the migration of keratinocytes from the edges of the wound and hair follicles, their proliferation, stratification, and differentiation/maturation to form the neo-epithelium (Woodley, 1996).

Address correspondence to Walter Wahli, Institut de Biologie Animale, Université de Lausanne, Bâtiment de Biologie, CH-1015 Lausanne, Switzerland. Tel.: (41) 21-692-41-10. Fax: (41) 21-692-41-15. E-mail: walter.wahli@iba.unil.ch

Pascal Escher's present address is Parke-Davis Pharmaceutical Research, Molecular Biology, Ann Arbor, MI 48105.

Jeffrey Peters' present address is Department of Veterinary Science, Center for Molecular Toxicology, Pennsylvania State University, 226 Fenske Laboratory, University Park, PA 16802.

Sharmila Basu-Modak's present address is Department of Pharmacy and Pharmacology, University of Bath, BA2 7AY Bath, United Kingdom.

Key words: mouse keratinocytes; PPAR gene expression; PPAR gene targeted disruption; skin wound healing; nuclear hormone receptors

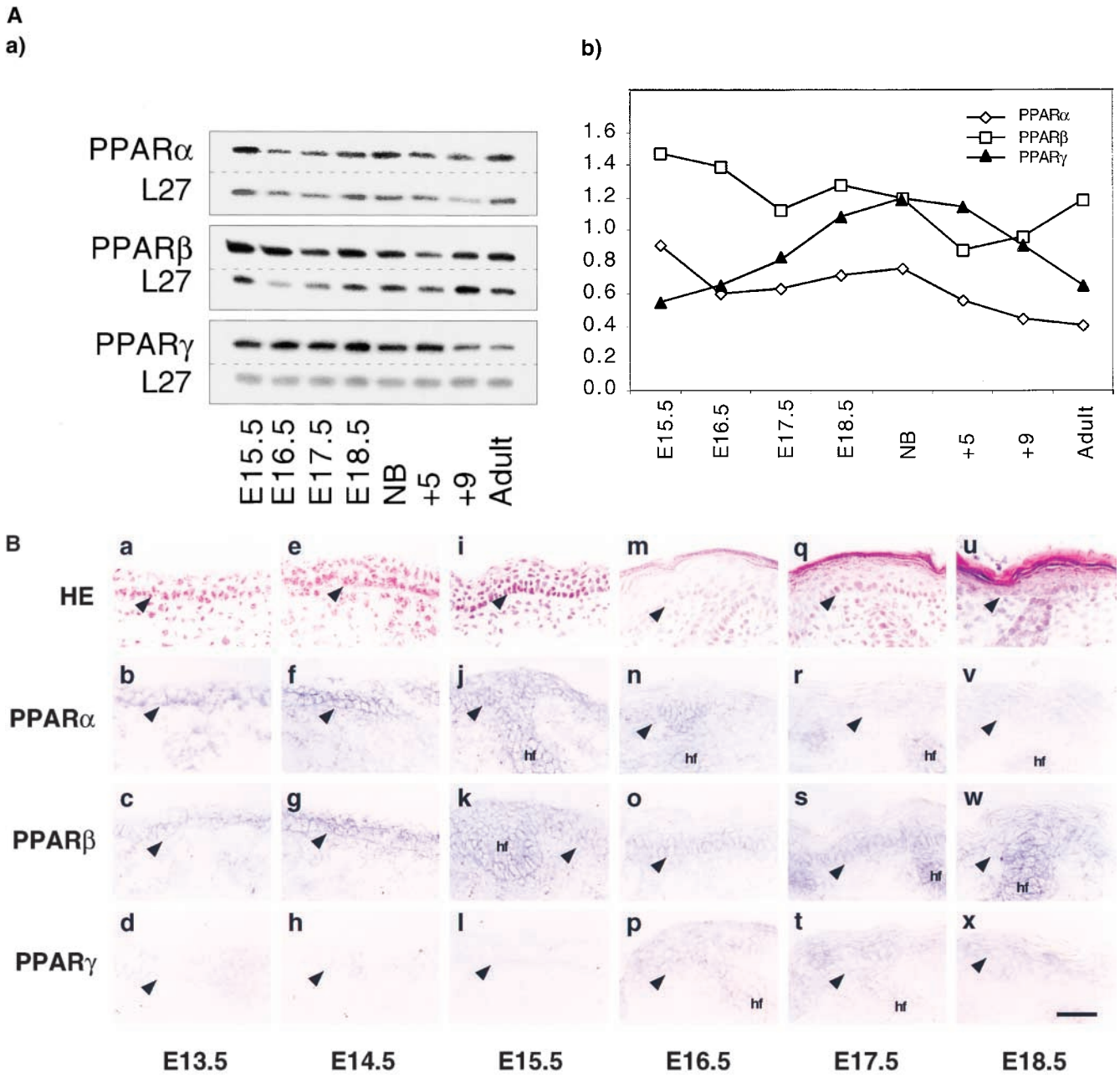

Figure 1. **Differential expression of the PPARs in mouse epidermis.** (A) RNase protection analysis of PPAR mRNA during mouse skin development. Total lysates of skin from day 15.5 to 18.5 embryos (E15.5–E18.5), newborn (NB), 5- and 9-d-old (+5, +9), and adult mice were hybridized with radiolabeled probes specific for PPARα, PPARβ, PPARγ, and L27 mRNA (a). The amount of mRNA for each PPAR isotype was quantified based on the L27 mRNA amount and on the specific activity of each probe (b; n = 3–6). (B) In situ hybridization analysis of PPAR expression during fetal development. Cryosections of mouse skin from embryonic day 13.5–18.5 (E13.5–18.5) were hematoxilin and eosin stained (HE) or hybridized with specific antisense digoxygenin–labeled riboprobes (PPARα, β, or γ). (C) In situ hybridization analysis of PPAR expression during post natal growth. Cryosections of mouse skin from newborn (NB), 5- or 9-d-old pups (+5, +9) and adult animals were hematoxilin/eosin stained (HE) or hybridized with specific antisense digoxygenin-labeled riboprobes (PPARα, β, or γ). Arrows indicate the epidermis/dermis interface. For both B and C, a similar pattern of expression was observed for each time point in five different mice from independent litters. Bars, 80 μm.

Among the various factors that influence skin maturation and development, many nuclear hormone receptors have been implicated. After binding of their respective ligands, nuclear hormone receptors activate the transcription of specific target genes. Various ligands for several members of the nuclear hormone receptor family are known to influence epidermis differentiation. Thyroid hormones and glucocorticoids accelerate the permeability barrier maturation of rat skin in vivo and in vitro (Aszterbaum et al., 1993; Hanley et al., 1996a, 1997a). Estrogen accelerates the skin barrier formation, whereas testosterone delays the process (Hanley et al., 1996b). Retinoids also influence the differentiation of the epidermis, even though the description of their functions are different when assayed in vitro or in vivo (Imakado et al., 1995; Saitou et al., 1995; Li et al., 2000, 2001). More recently,

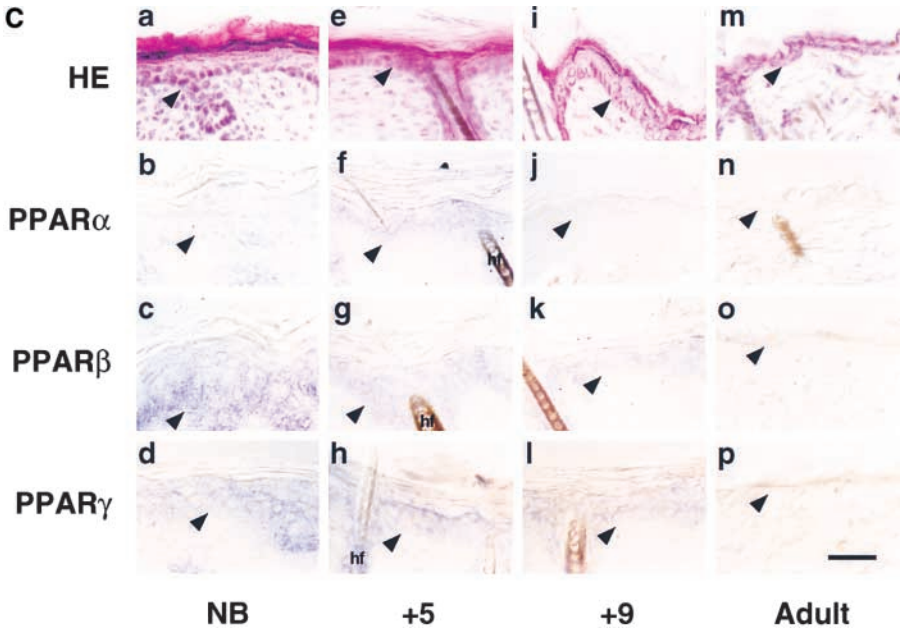

Figure 1 (continued).

peroxisome proliferator–activated receptor (PPAR)* and farnesol X–activated receptor ligands were shown to accelerate epidermal development when added to fetal rat skin explants, whereas PPARγ ligands have no effect (Hanley et al., 1997b, 1998). The situation seems to be different in human keratinocytes, since only a PPARβ-selective ligand, but not PPARα or γ ligands, induced the expression of keratinocyte differentiation markers (Westergaard et al., 2001). In addition, recent results suggested that a cross talk exists between the PPAR and the cholesterol metabolism pathways in the epidermis (Hanley et al., 2000).

The subfamily formed by the PPARs binds fatty acids and their derivatives as well as hypolipidemic and antidiabetic agents and plays important roles in energy homeostasis. Three isotypes have been identified (PPARα, β/δ or FAAR or NUC1, and γ; NR1C1, NR1C2, NR1C3, respectively; Nuclear Receptor Nomenclature Committee, 1999) in various species (*Xenopus* laevis, rodents, human), each of them having a specific pattern of expression (for review see Desvergne and Wahli, 1999).

Consistent with a potential role of PPAR ligands in epidermis maturation, PPARs are expressed both in rat skin and human keratinocytes (Braissant et al., 1996; Braissant and Wahli, 1998; Rivier et al., 1998). In skin, RNase protection assay and in situ hybridization reveals that PPARα and PPARβ are both expressed in the epidermis during embryogenesis. However, no major skin defect has been described in PPARα null mice, suggesting that PPARα is not essential for skin maturation in rodents (Lee et al., 1995). In contrast, we show in this study that PPARα and PPARβ are crucial for rapid skin repair in the adult animal.

*Abbreviations used in this paper: AS, antisense; K6, keratin 6; PPAR, peroxisome proliferator–activated receptor; RPA, ribonuclease protection assay; S, sense; TPA, tetradecanoylphorbol acetate.

Results

PPAR gene expression in the epidermis

PPAR gene expression in the mouse skin was analyzed by RNase protection assay from day 15.5 of gestation until adulthood (Fig. 1 A). Total skin extracts, including the epidermis and the dermis, were prepared and PPAR mRNA levels were analyzed using radiolabeled PPARα-, β-, and γ-specific probes. The three PPAR isotypes were found to be expressed both in embryonic and in postnatal developing skin at all the stages analyzed (Fig. 1 A). Normalization (L27 and specific activities of the probes) and quantification of the results revealed that PPARα is the least abundant isotype during development, except at embryonic day 15.5. The level of expression of PPARβ, which is ~1.5 higher than PPARα at E15.5, steadily decreases until after birth. At day 15.5 of gestation, PPARγ is the least expressed PPAR isotype (1.5 and 2–3 times lower than PPARα and PPARβ, respectively). After a twofold increase during late embryonic development, the PPARγ expression level decreases in the postnatal period. In the adult skin, PPARα and PPARγ are low, with PPARβ remaining the highest expressed isotype.

To precisely localize PPAR expression in the skin, the tissue pattern of expression of the three PPAR isotypes was assessed on mouse skin section using in situ hybridization with specific PPARα, β, and γ digoxigenin–labeled probes. During fetal development from embryonic day 13.5 on to the end of the gestation, the three PPAR isotypes were expressed, generally at relatively low levels, in the differentiating epidermis and hair follicles (Fig. 1 B). PPARα and β were found to be expressed in the dermis as well, although at lower levels compared with the epidermis. PPARα, β, and γ were still expressed in the epidermis of newborn pups (Fig. 1 C), but their expression in the interfollicular epidermis decreased after a few days of postnatal development. In the adult mouse skin, no expression could be detected for any of the three isotypes in the interfollicular epidermis (Fig. 1 C), whereas they were still highly expressed in the hair follicle keratinocytes (not shown).

Table I. **Induced keratinocyte proliferation after TPA topical application or hair plucking**

	PPARβ+/+		PPARβ+/−	
Control				
Mean epidermal thickness	10.8 ± 0.31	100%	12.62 ± 0.25[a]	100%
Ki67 labeling	11.1 ± 1.1	100%	14.2 ± 1.0	100%
TPA application				
Epidermal thickness	26.1 ± 1.3[a]	230.6 ± 10.4[b]	32.3 ± 2.4[b]	271.5 ± 18.2[b]
Ki67 labeling	24.3 ± 1.3[b]	219.2 ± 12.6	31.7 ± 1.7[b]	223.4 ± 12.5
Hair plucking				
Epidermal thickness	19.9 ± 0.5[a]	183.9 ± 8.3[a]	29.9 ± 2.0[a]	237.0 ± 16.0[a]
Ki67 labeling	18.6 ± 1.3[a]	167.6 ± 12.2	24.1 ± 0.9[a]	169.5 ± 6.9

Mean epidermal thickness was measured via light microscopy using the Object Image software. Absolute (μm) and relative values (% control) are both shown (± SEM, five microscopic fields, five different animals). The number of Ki67-positive cells was also measured using the Object Image software. Absolute (number of Ki67-positive cells) and relative values (% control) are both shown (± SEM, five microscopic fields, five different animals).
[a]Based on the Student's t test, the difference is statistically significant (P , 0.01).
[b]Based on the Student's *t* test, the difference is statistically significant ($P < 0.05$).

Thus, in situ hybridization revealed that the expression of the PPARs in the adult skin, measured by ribonuclease protection assay (RPA), is mainly due to their presence in the hair follicles, whereas they are undetectable in the interfollicular epidermis. The pattern of expression of PPAR in the epidermis at embryonic and adult stage suggests that the presence of the PPARs in the keratinocytes is related to proliferation and/or differentiation during development, rather than to the normal adult epidermis renewal.

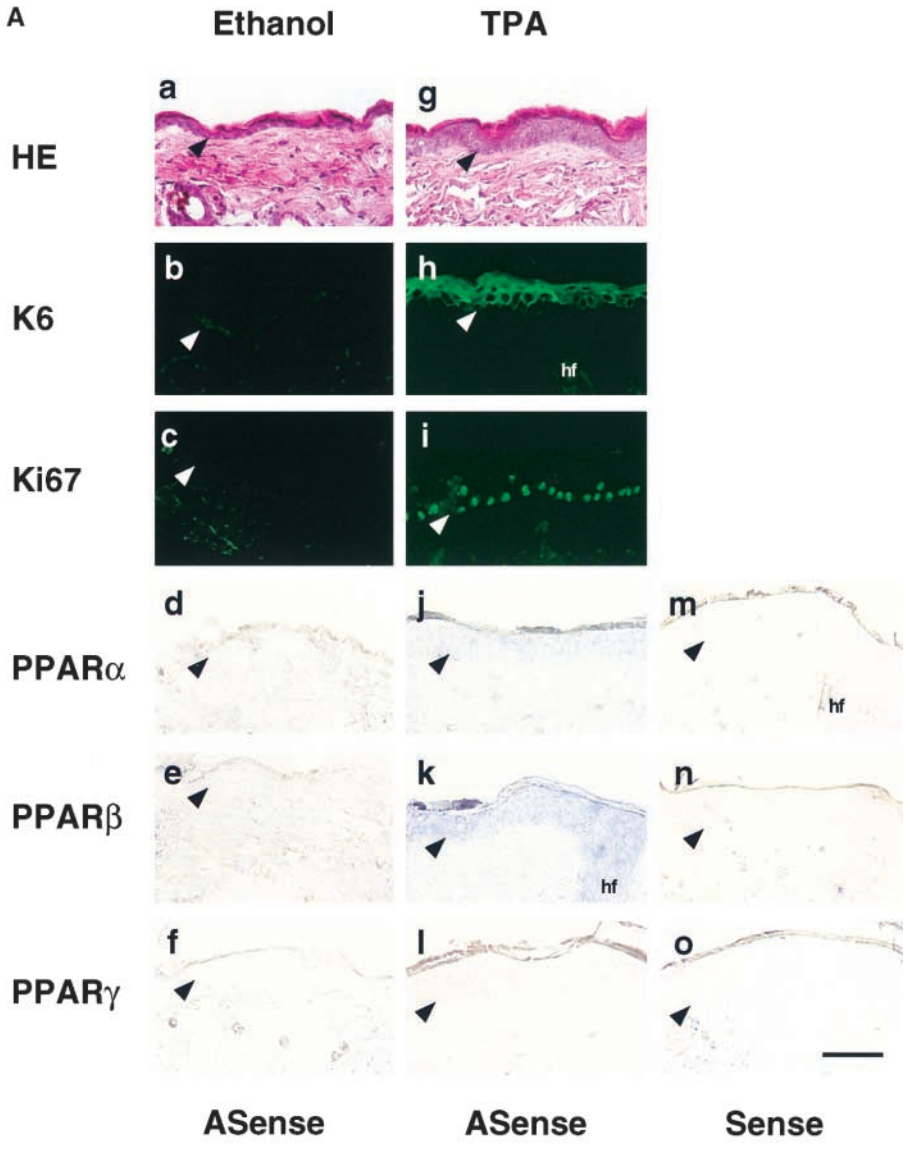

Figure 2. **PPARβ expression is upregulated in SV129 adult mouse epidermis upon keratinocyte proliferation stimulation.** TPA topical application. Vehicle- (a–f) or TPA-treated (g–l) dorsal skin. Hematoxilin/eosin (HE) staining (a and g); Keratin 6 (b and h) and Ki67 (c and i) immunolabeling; in situ hybridization with PPARα (d and j), PPARβ (e and k), and PPARγ (f and l) antisense probes (ASense); in situ hybridization of TPA-treated samples with sense control probes are shown (m–o). (B) Hair plucking. Unplucked (a–f) or plucked (g–l) dorsal skin. Hematoxilin/eosin (HE) staining (a and g); Keratin 6 (b and h) and Ki67 (c and i) immunolabeling; in situ hybridization with PPARα (d and j), PPARβ (e and k), and PPARγ (f and l) antisense probes (ASense); in situ hybridization of plucked samples with sense control probes are shown (m–o). Arrows indicate the epidermis/dermis interface. For both A and B, similar results were observed in six SV129 mice from independent litters. Bars, 80 μm.

PPARβ expression is upregulated in vivo upon stimulation of keratinocyte proliferation

To address the hypothesis that the expression of PPARs in the epidermis is related to keratinocyte proliferation, we looked at their expression in the adult mouse epidermis after stimulation of keratinocyte proliferation either by topical application of tetradecanoylphorbol acetate (TPA) or by hair plucking. If PPARs are involved in keratinocyte proliferation and/or differentiation, their expression might be reactivated by these stimuli.

TPA applied on the dorsal skin of SV129 mice induced thickening of the epidermis within 48 h, whereas no change was observed on the vehicle-treated control samples. Histological staining of the TPA-treated skin showed a typical increase in keratinocyte stratification compared with the control (Fig. 2 A, and Table I). As markers for keratinocyte proliferation, we used the expression of both keratin 6 (K6) cytoskeletal protein (Navarro et al., 1995) and the Ki67 nuclear antigen. As shown in Fig. 2 A, K6 immunolabeling remained negative in the ethanol-treated control epidermis, whereas high levels were detected in the epidermis after TPA application, confirming that this agent induced the expected proliferation of the keratinocytes. Consistent with this, the number of Ki67-positive cells in the basal layer was also increased in the TPA-treated samples (Fig. 2 A, and Table I). In situ hybridization with PPARα-, β-, and γ-specific probes revealed that PPARβ expression was significantly upregulated in the TPA-treated epidermis, whereas only a faint signal was detected for PPARα and no signal for PPARγ (Fig. 2 A). Consistent with the results shown in Fig. 1 C, none of the three PPAR isotypes was detected in the interfollicular epidermis of the control sample.

In a second approach, hairs from a small surface of dorsal skin of SV129 mice were gently plucked, and the proliferative effect on keratinocytes was checked by histological staining, K6 and Ki67 immunolabeling (Fig. 2 B). In contrast to the unplucked control skin, the epidermis of the plucked surface showed both an increased stratification of the keratinocytes and a strong induction of Ki67 and K6 expression (Fig. 2 B, and Table I). Similar to TPA treatment, PPARβ expression was markedly upregulated as a result of hair plucking, whereas PPARα showed only a weak increase

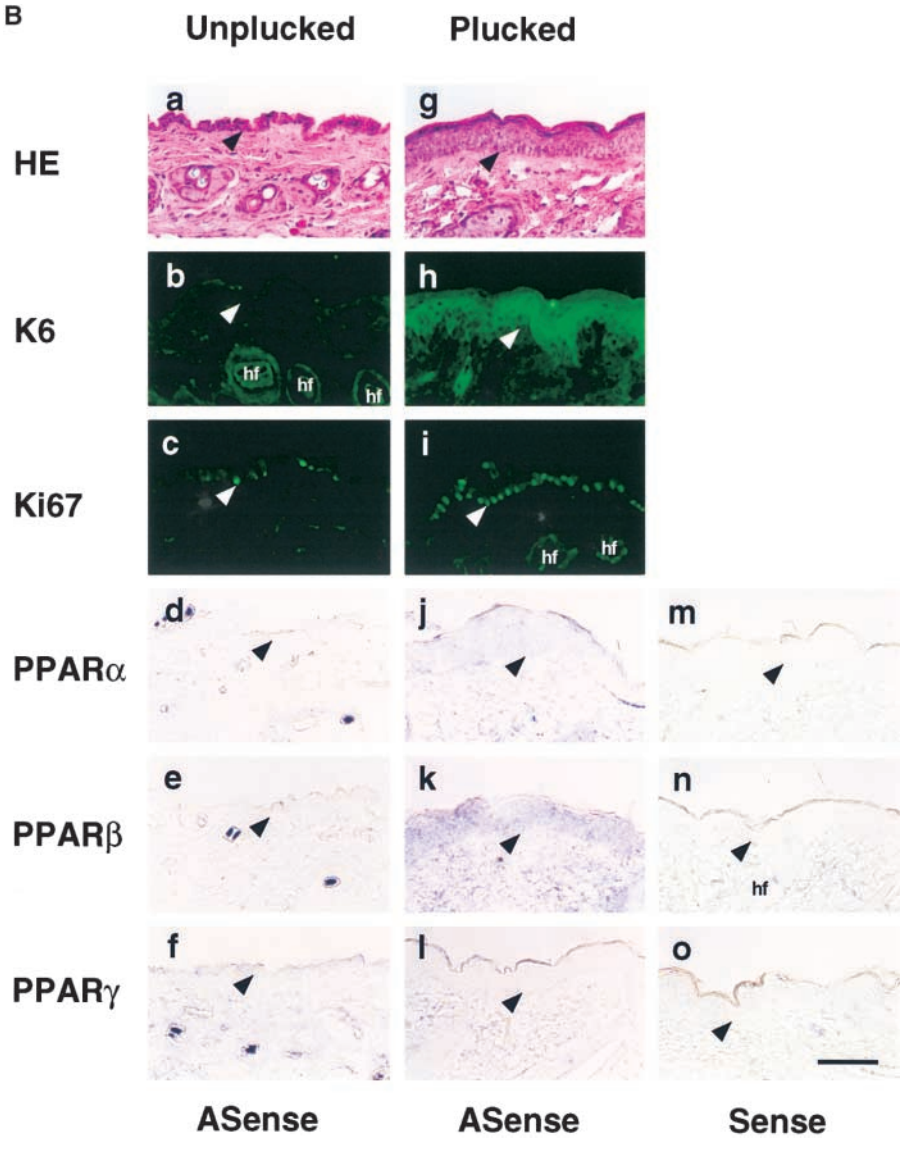

Figure 2 (continued).

Table II. **PPAR expression level in PPARβ and PPARγ mutant mouse lines**

	Brain		Kidney		Liver	
	PPARβ+/+	**PPARβ+/−**	**PPARβ+/+**	**PPARβ+/−**	**PPARβ+/+**	**PPARβ+/−**
PPARα RNA	NA	NA	0.33	0.29	0.29	0.30
PPARβ RNA	0.67 (100%)	0.33 (49.2%)	0.51 (100%)	0.29 (56.8%)	0.25 (100%)	0.18 (72%)
PPARβ protein	1.2 (100%)	0.51 (42.5%)	13.0 (100%)	5.8 (44.6%)	8.1 (100%)	4.1 (50.6%)
PPARγ RNA	NA	NA	0.013	0.018	0.012	0.018
	Liver		**Muscle**		**WAT**	
	PPARγ+/+	**PPARγ+/−**	**PPARγ+/+**	**PPARγ+/−**	**PPARγ+/+**	**PPARγ+/−**
PPARα RNA	0.39	0.31	0.064	0.064	NA	NA
PPARβ RNA	0.26	0.28	0.071	0.071	0.162	0.136
PPARγ RNA	0.017 (100%)	0.007 (41.2%)	0.011 (100%)	0.006 (54.5%)	1.175 (100%)	0.696 (59.2%)
PPARγ protein	NA	NA	NA	NA	2.6 (100%)	1.1 (42.3%)

Table II shows the quantification of PPARα, β, and γ RNA and of PPARβ and PPARγ protein levels in the PPARβ and PPARγ mutant mouse lines, respectively. The results represent the normalized values obtained after quantification of the RNase protection assays and Western blots (not shown). In parentheses: percentage decrease of PPARβ and PPARγ expression compared to the wild-type control samples (100%) in the PPARβ and PPARγ mutant mouse lines, respectively.

and PPARγ remained undetectable as analyzed by in situ hybridization.

Thus, the marked increase in PPARβ expression under conditions inducing keratinocyte proliferation and stratification provides a strong indication that PPARβ might be directly implicated in these processes.

Generation of PPARβ and γ mutant mice

To study each PPAR function in the skin in vivo, we used PPAR mutant mice. The PPARα null mouse has been described previously (Lee et al., 1995) and we generated PPARβ and PPARγ mutant animals (unpublished data). Early embryonic lethality of PPARγ null mutants was observed, as also reported recently by others (Barak et al., 1999; Kubota et al., 1999). Similarly, due to incomplete but very high penetrance of a lethal phenotype, only few PPARβ null mice could be obtained but no null mice line could be established so far. Similar difficulties in generating PPARβ homozygous null animals was also described recently by Peters et al. (2000); although, in that case, a PPARβ knock out line was finally obtained on a different genetic background. Therefore, and due to the above-mentioned difficulties in obtaining homozygous null mice, we used heterozygous PPARβ and PPARγ mice in our experiments.

For each mouse line, the PPAR mRNA and protein levels were analyzed by RNase protection assay and Western blot. The amounts of PPARβ and PPARγ mRNA and protein are decreased by half in the PPARβ and PPARγ+/− mice, respectively, with no compensation by the other PPAR isotypes (Table II and data not shown).

Increased keratinocyte proliferative response in PPARβ+/− mice

To test the hypothesis of a PPARβ implication in the control of keratinocyte proliferation, we used the above mentioned PPARβ+/− mutant mice. As shown in Fig. 3 A, these heterozygous mice showed a normal skin architecture upon histological staining. However, a careful examination of the epidermal thickness and of the keratinocyte proliferation rate indicate a slight but significant increase of both parameters in the PPARβ+/− mice compared with the wild-type control animals (Table I). Thus, if PPARβ and keratinocyte proliferation are linked, the latter might be affected in the mutant heterozygous animals after proliferation stimuli. Therefore, we performed a TPA stimulation on the dorsal epidermis of PPARβ+/− and control wild-type mice. As shown in Fig. 3 A, a hyperplasia of the TPA-treated epidermis occurred as expected in control mice. Compared with the wild-type control, the PPARβ+/− mice showed a more pronounced stratification of the epidermis. Confirming the morphological observation, the K6 and Ki67 induction in the epidermis was higher in the PPARβ mutant mice than in the wild-type animals (Fig. 3 A, and Table I). The higher proliferative response of the keratinocytes in the epidermis of the PPARβ+/− mice was also observed after hair plucking of the dorsal skin (Fig. 3 B, and Table I). Thus, in both assays, the proliferative response of the keratinocytes was significantly higher in the heterozygous mice compared with the wild-type control (Table I). These data provide further evidence for PPARβ involvement in the control of keratinocyte proliferation. PPARα, on the contrary, does not seem to be involved in this mechanism, as the TPA stimulation on dorsal skin induced identical epidermis hyperplasia in both PPARα wild-type control and PPARα−/− mice (data not shown).

Epidermal differentiation and hair follicle cycle are not affected in PPARβ+/− mice

Because PPARβ is expressed in the epidermis during fetal and postnatal development (Fig. 1), and because of its involvement in the control of keratinocyte proliferation (Fig. 3), the question was raised whether the differentiation process would also be affected in the epidermis of PPARβ mutant mice. To address this question, the skin morphology and the pattern of expression of several keratinocyte differentiation markers (keratins 14 and 10, loricrin, involucrin) were analyzed in the epidermis of PPARβ mutant mice from day 14.5 of gestation until adulthood. As shown after histological staining, the PPARβ mutant mice show normal skin architecture, both during fetal development (embryonic day 14.5 and 16.5, data not shown; embryonic day 18.5, Fig. 4) and at the adult stage (Fig. 4). Immunofluorescent labelings revealed that the pattern and the time course of expression of

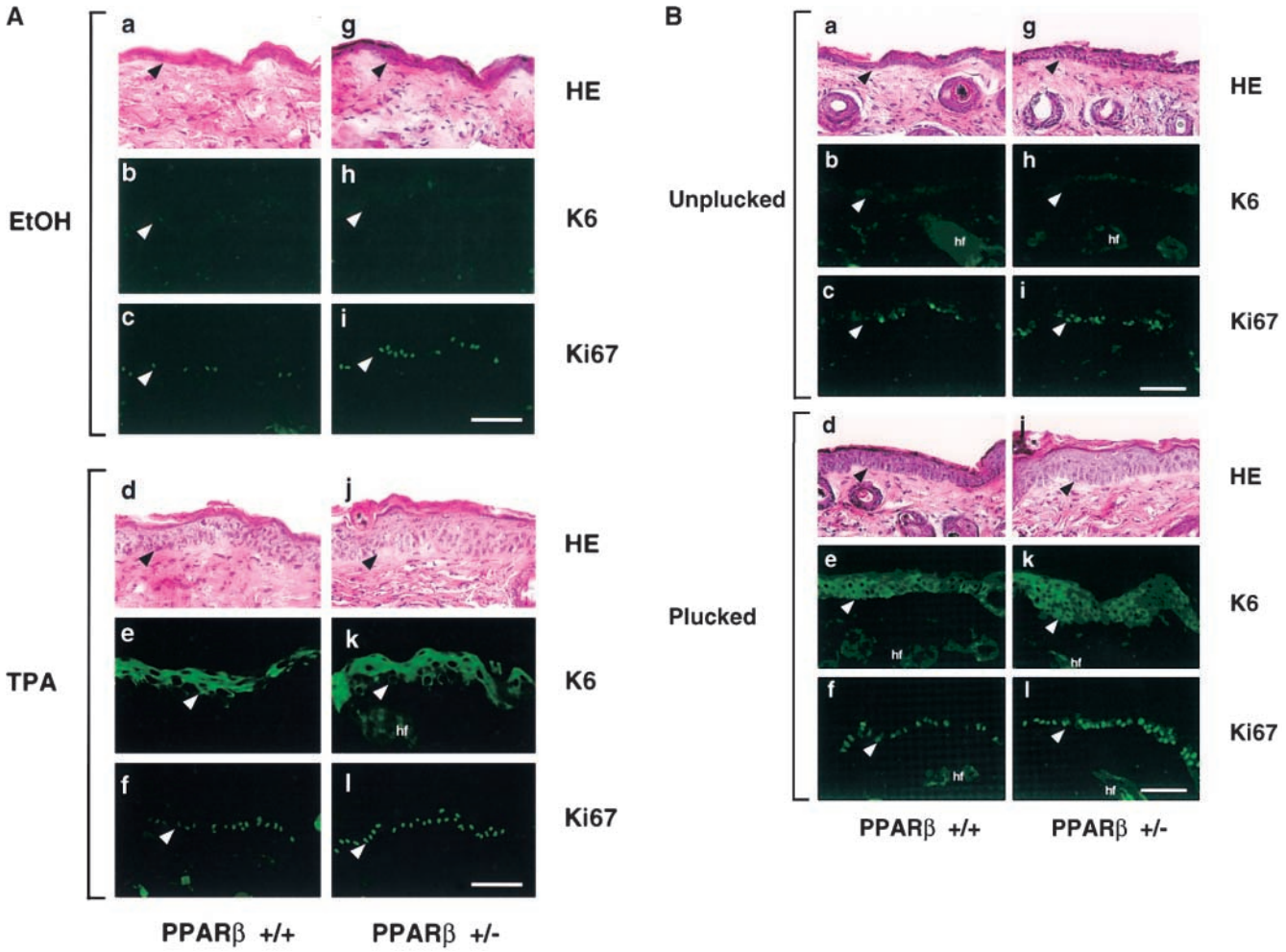

Figure 3. **Enhanced keratinocyte proliferative response in PPARβ+/− upon stimulation.** (A) TPA topical application. (a–f) PPARβ+/+ vehicle (a–c) or TPA-treated (d–f) dorsal epidermis, hematoxilin/eosin staining (HE) (a and d), and after keratin 6 (b and e) or Ki67 (c and f) immunostaining. (g–l) PPARβ+/− vehicle– (g–i) or TPA-treated (j–l) dorsal epidermis, hematoxilin/eosin staining (HE) (g and j), and after keratin 6 (h and k) or Ki67 (i and l) immunostaining. (B) Hair plucking. (a–f) PPARβ+/+ unplucked (a–c) or plucked (d–f) dorsal epidermis, hematoxilin/eosin staining (HE) (a and d), and after keratin 6 (b and e) or Ki67 (c and f) immunostaining. (g–l) PPARβ+/− unplucked (g–i) or plucked (j–l) dorsal epidermis, hematoxilin/eosin staining (HE) (g and j), and after keratin 6 (h and k) or Ki67 (i and l) immunostaining. Arrows indicate the epidermis/dermis interface. Bars, 80 μm.

the above mentioned differentiation markers was similar in the PPARβ mutant and the wild-type control epidermis (Fig. 4 and data not shown).

Since PPARβ is present in the hair follicle during fetal development and remains highly expressed in this epithelial appendage at the adult stage, the hair follicle cycle was compared between PPARβ heterozygous and wild-type mice in unchallenged skin and after hair plucking. Similarly to the expression of differentiation markers, no defect was observed in the hair growing or in the structure of the hair follicles of PPARβ mutant mice (data not shown).

These observations suggest that one functional PPARβ allele is sufficient to maintain normal fetal and postnatal epidermal development in the PPARβ mutant mice, or that PPARs may have redundant functions in terms of epithelial differentiation.

PPAR gene expression in a wounded epidermis

In addition to the link between PPARβ and keratinocyte proliferation, the expression patterns of the three PPAR isotypes suggest that they are most likely associated with epidermal fetal maturation. Thus, we studied PPAR expression during skin wound healing, an extreme situation in which the adult skin has to regenerate a neoepidermis. This epidermal repair includes both hyperproliferation of the keratinocytes and differentiation of a new epithelium upon closure of the wound.

A half centimeter square, full thickness skin biopsy was excised from the back of adult mice, and PPAR expression was assessed by in situ hybridization at several time points after the injury at the site of the wound (Fig. 5). In situ hybridization revealed that PPARα and PPARβ are both upregulated in the epidermis of the wound edges, compared with a normal adult epidermis where they cannot be detected. PPARβ reactivation was detected as early as 24 h after the injury. Furthermore, it remained expressed in the epidermis of the wound edges and in the neoepithelium during the whole healing process. After closure of the wound, PPARβ was downregulated and it became undetectable 20 d after injury. In contrast, PPARα expression was observed during a short

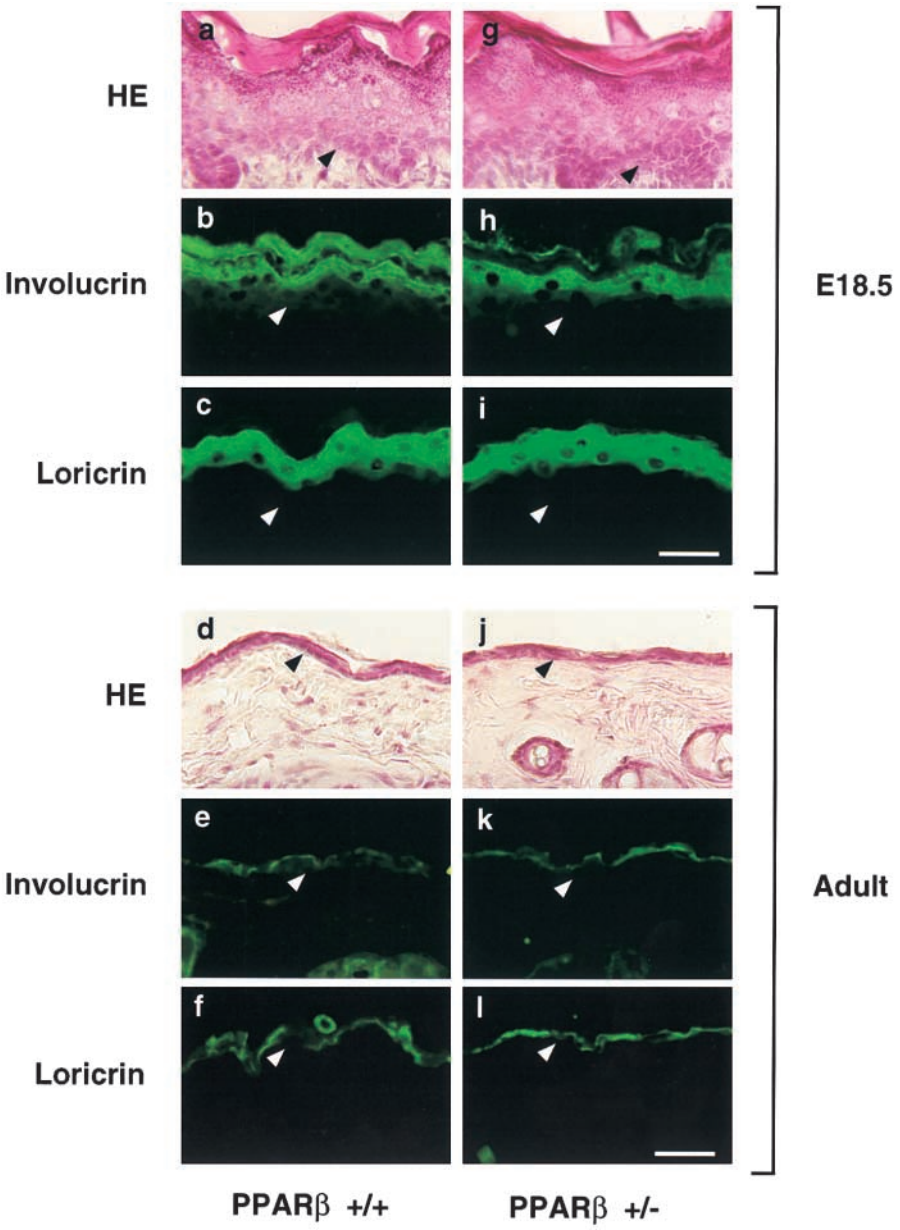

Figure 4. **Normal keratinocyte-terminal differentiation in PPARβ+/− skin.** (a–f) PPARβ+/+ fetal (E18.5) (a–c) or adult (d–f) dorsal epidermis, hematoxilin/eosin staining (HE) (a and d), and after involucrin (b and e) or loricrin (c and f) immunostaining. (g–l) PPARβ+/− fetal (E18.5) (g–i) or adult (j–l) dorsal epidermis, hematoxilin/eosin staining (HE) (g and j), and after involucrin (h and k) or loricrin (i and l) immunostaining. Arrows indicate the epidermis/dermis interface. Bars, 40 μm.

period of time only, ~3 d after the injury, and was not observed thereafter. The third isotype, PPARγ, was hardly detectable, which suggests modest or no implication of this isotype in the skin wound–healing process.

The differential upregulation of both PPARα and β in the epidermis of the wound edges suggests that each of them may play a specific role during the wound-healing process.

PPARα−/− and β+/−, but not PPARγ mutant mice, exhibit altered skin wound healing

The respective roles of PPARα, β, or γ during cutaneous wound healing were assessed by measuring the efficiency of the healing of a full thickness wound in PPARα, β, or γ mutant mice.

As described above, a dorsal skin biopsy was excised on adult mice, the surfaces of the wounds were measured until complete healing, and the effect of either the PPARα, β, or γ mutation was addressed by comparing the kinetics of wound healing in transgenic and normal littermates. In all the mice, either transgenic or wild-type controls, the reepithelialization was preceded by the formation of a scab, decrease of the wound surface, and loss of the scab upon healing of the wound. A significant degree of strain variability was observed in the wound closure kinetics of the control animals of the three strains of mice. This observation is in agreement with reports on healing of skin wounds, in which initial closure (1 d after the biopsy) of wild-type control animals varied from 10–60%, depending on the mouse strain (Kaya et al., 1997; Crowe et al., 2000; Gallucci et al., 2000; Streit et al., 2000; Echtermeyer et al., 2001). Due to this variation, only the differences in wound healing between mutant and their wild-type counterparts of each strain has been analyzed.

The PPARγ+/− heterozygous mice were not different from wild-type littermates in their wound-healing process

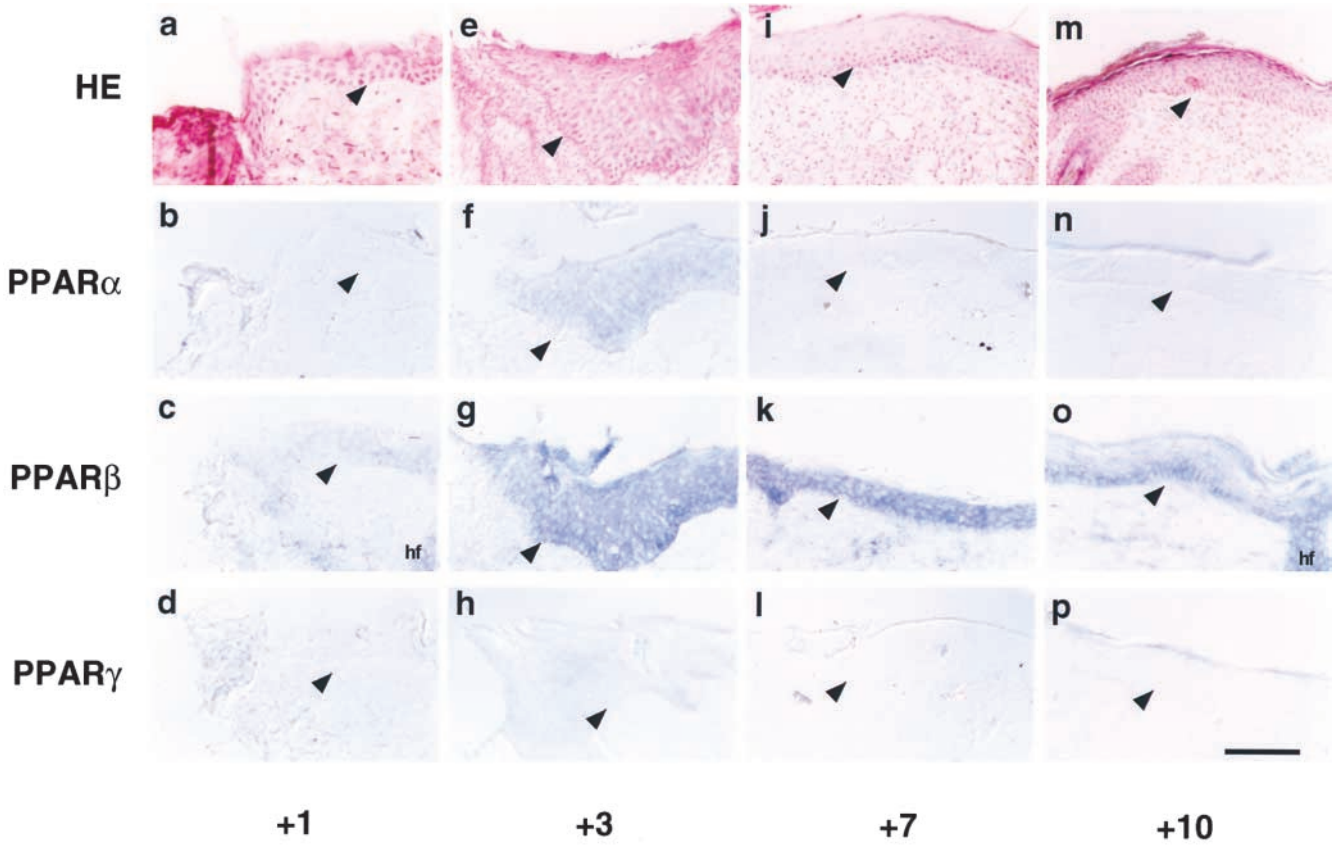

Figure 5. **Differential expression of PPAR in adult mouse epidermis during cutaneous wound closure.** Cryosections of mouse skin from day 1 to 10 (+1 to +10) after the excision of a full thickness dorsal skin biopsy were hematoxilin/eosin stained (HE) or hybridized with specific antisense digoxygenin-labeled riboprobes (PPARα, β, or γ). Arrows indicate the epidermis/dermis interface. A similar pattern of expression was observed for each time point in six different mice from independent litters. Bar, 80 μm.

(Fig. 6 A), which is consistent with PPARγ being hardly detectable after injury.

Compared with their wild-type counterparts, PPARα−/− mice showed a delay in wound healing during the first 4 d after injury (Fig. 6 B), as the surface of the wounds on the PPARα−/− mice decreased more slowly than for the wild-type control mice. The healing efficiency was then restored and the resolution of the healing process finally happened within the same delay in both control and null mice. This difference in the healing efficiency was observed both with young (6–8 wk) and old (12–18 mo) mice, suggesting that the phenotype is independent of the age of the animals. Additionally, a similar phenotype was observed in mice expressing a PPARα dominant negative transgene specifically in the epidermis (unpublished data). Interestingly, the initial and transient delay observed for the healing of the PPARα null mice correlates with the window of PPARα-increased expression during the tissue repair process, and corresponds to the inflammatory phase of wound healing (see Figs. 5, 6 B, and 7). Therefore, we assessed the inflammatory infiltration in PPARα+/+ and −/− mice by quantification of the number of neutrophils and monocytes/macrophages present in the wound bed at day 1, 3 and 5 postwounding. As shown in Table III, both the recruitment of neutrophils and monocytes is impaired in the PPARα−/− at day 1 postwounding. The difference in the recruitment of these immune cells disappears after a few days, allowing for the restoration of normal repair in the PPARα−/− mice.

The healing kinetics obtained with the PPARβ+/− heterozygous mice were different from the one described above for PPARα−/− mice. The healing of the PPARβ+/− mice was delayed during the whole repair process compared with their wild-type littermates (Fig. 6 C), and final closure was postponed by 2–3 d. With respect to the cascade of events implicated in the closure of a skin wound (Fig. 7), a delay

Table III. **Inflammatory infiltrate in the wound bed of PPARα wild-type and null mice**

Day postwounding	Neutrophil number		Monocyte/macrophage number	
	PPARα+/+	PPARα−/−	PPARα+/+	PPARα−/−
1	76.1 ± 5.5	63.6 ± 2.5[a]	12.4 ± 0.8	27.8 ± 3.1[b]
3	50.3 ± 6.0	40.5 ± 3.4	51.2 ± 2.8	54.4 ± 2.1
5	16.1 ± 2.2	11.6 ± 1.0	50.0 ± 3.3	47.7 ± 2.5

The number of neutrophils and of monocytes/macrophages present in the wound bed at day 1, 3, and 5 postwounding was assessed based on morphological criteria in PPARα wild-type and null mice. The values represent the mean of the number of cells counted in five standardized microscope fields per section, performed on three different animals for each stage postwounding, ± SEM.
[a]Based on a Student's *t* test, the difference is statistically significant ($P < 0.05$).
[b]Based on a Student's *t* test, the difference is statistically significant ($P < 0.01$).

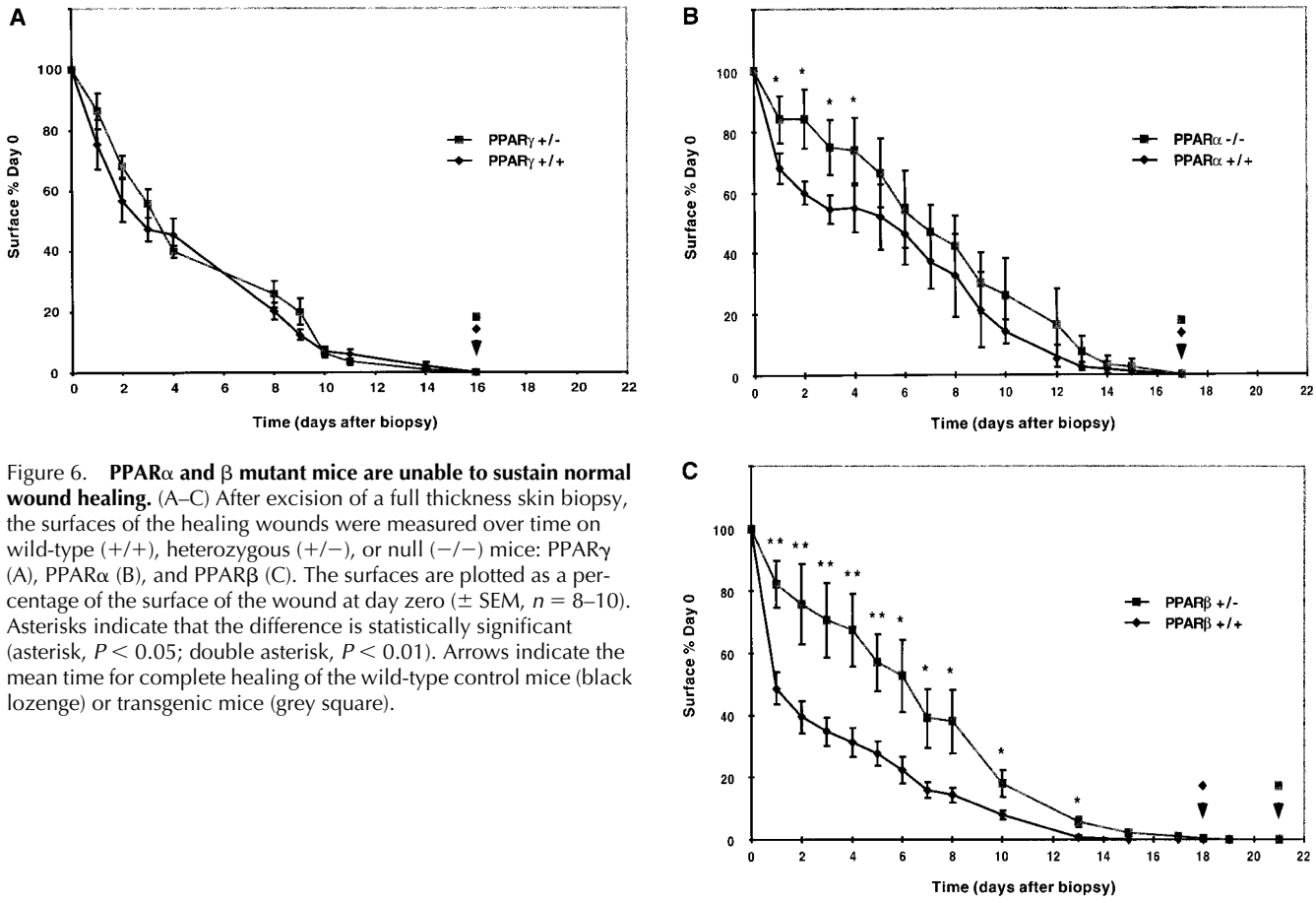

Figure 6. **PPARα and β mutant mice are unable to sustain normal wound healing.** (A–C) After excision of a full thickness skin biopsy, the surfaces of the healing wounds were measured over time on wild-type (+/+), heterozygous (+/−), or null (−/−) mice: PPARγ (A), PPARα (B), and PPARβ (C). The surfaces are plotted as a percentage of the surface of the wound at day zero (± SEM, $n = 8–10$). Asterisks indicate that the difference is statistically significant (asterisk, $P < 0.05$; double asterisk, $P < 0.01$). Arrows indicate the mean time for complete healing of the wild-type control mice (black lozenge) or transgenic mice (grey square).

observed during the whole process suggests either a default in skin elasticity and contraction of the wound, or an impaired keratinocyte migration/proliferation. To test the first possibility, elastin- and collagen-specific stainings and dorsal incisional wounds were made on PPARβ+/− and wild-type mice. In unchallenged adult skin, the elastin and collagen deposits were similar in the PPARβ wild-type and mutant dermis (Fig. 8). Moreover, the time course of collagen accumulation in the granulation tissue during the healing of a wound is identical in the PPARβ+/− mice compared with the wild-type controls (Fig. 8). Finally, the incisional wounds remained perfectly linear in both genotypes, indi-

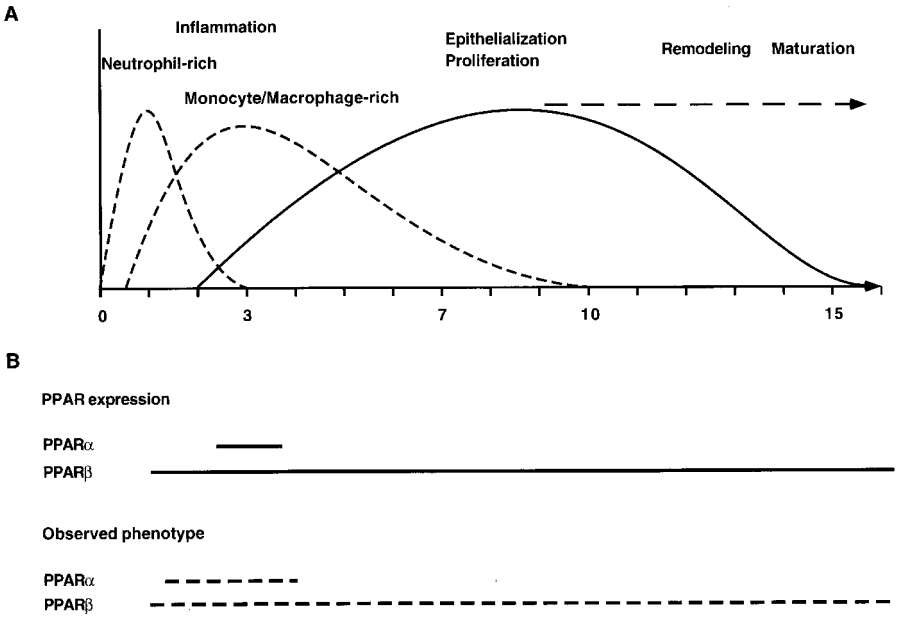

Figure 7. **PPAR α and β expression and respective mice phenotypes compared with the major phases of skin wound healing.** (A) Summary of time sequence of the major overlapping phases of skin wound healing. (B) Plain lines indicate the expression of PPARα and β in the healing epidermis; dotted lines indicate the duration of the observed phenotype on PPAR mutant mice.

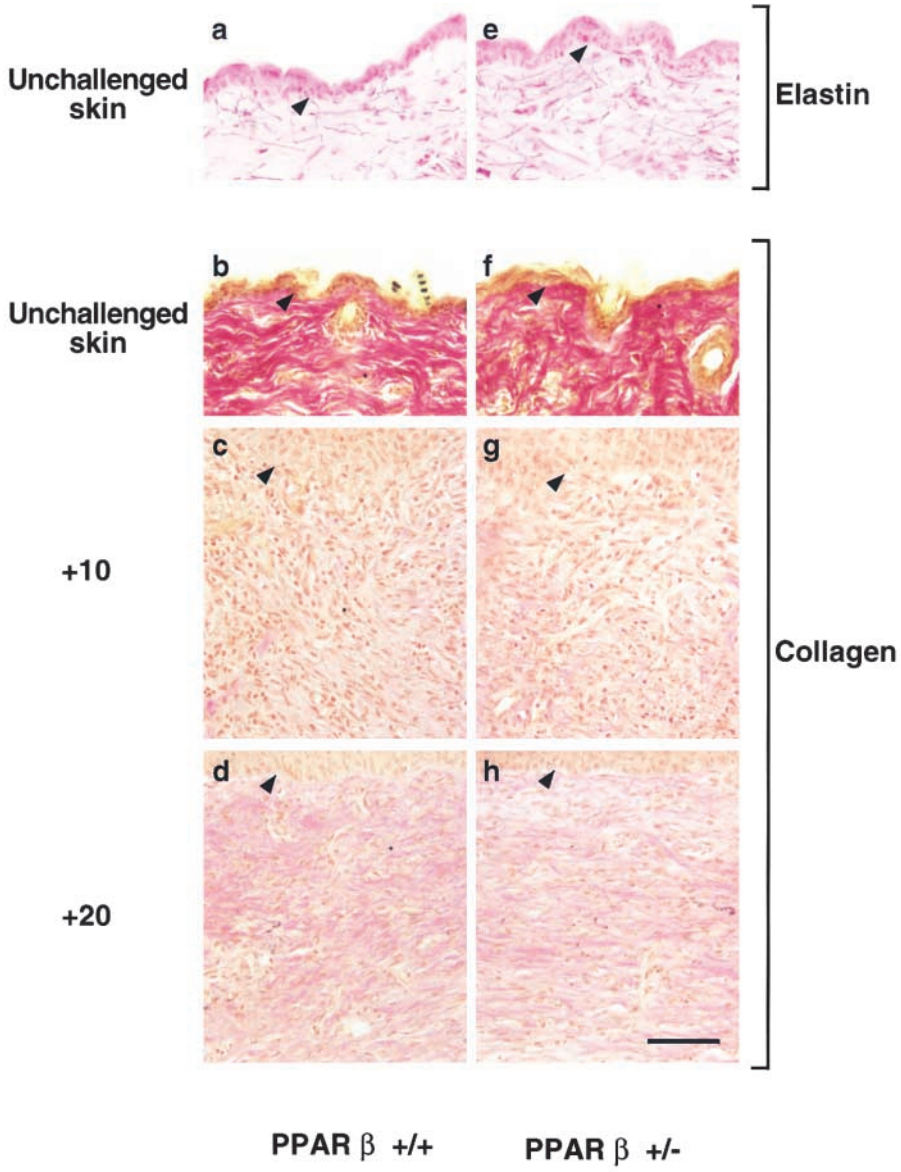

Figure 8. **Elastin and collagen deposit is not altered in the dermis of PPARβ+/− mice.** PPARβ+/+ (a–d) or PPARβ+/− (e–h) dorsal epidermis, elastin (a and e), or collagen (b–d and f–h) staining. (a, b, e, and f) Unchallenged adult dorsal skin. (c, d, g, and h) Mouse skin at day 10 and 20 (+10 and +20) after the excision of a full thickness dorsal skin biopsy. Arrows indicate the epidermis/dermis interface. Bar, 80 μm.

cating that skin elasticity is not impaired in the heterozygous mice (data not shown) and that the healing delay is not due to a loss of skin elasticity in the mutated animals.

Since the hypothesis of a defect in PPARβ+/− skin elasticity was unlikely, the adhesion and migration capacities of the PPARβ-mutated keratinocytes were studied in vitro using primary keratinocyte cultures. Keratinocytes were isolated from the skin of wild-type and PPARβ+/− newborn pups. PPARβ mutant keratinocytes in culture immediately showed impaired adhesion capacities: they adopted a rounded shape and only adhered 4 d after seeding, whereas the wild-type primary keratinocytes spread and adhered easily 24 h after seeding (Fig. 9). However, despite this adhesion defect and delay in adherence, the PPARβ mutant keratinocytes remain viable. Seeding of more mutant keratinocytes compared with the wild-type cells (see Materials and methods) allowed us to obtain 70–80% confluent cultures for both keratinocyte genotypes, allowing the study of in vitro healing of a scraping wound. After scraping of the culture, the wild-type and mutant cells behaved very differently at the edges of the in vitro wound. As shown in Fig. 9, the PPARβ wild-type keratinocytes remained in tight contact with each other and scraping resulted in folds at the edges (Fig. 9 b). On the contrary, the PPARβ+/− keratinocytes were easier to detach, and the produced edges were blunt (Fig. 9 f). Once the PPARβ wild-type keratinocytes started to migrate out of the edges, their migration rate was higher compared with that of the PPARβ+/− keratinocytes (Fig. 9, c, d, g, and h). This in vitro result indicates that the migration properties of the PPARβ mutant keratinocytes are impaired, consistent with observations in whole animal. Indeed, in vivo, the number of keratinocytes per surface unit is slightly higher at the edges of skin wound in the PPARβ mutant animals compared with the wild-type mice, also indicating that in vivo as well, the migration is slower in PPARβ mutant cells (data not shown).

In conclusion, mice with a mutated PPARα or β gene cannot sustain normal cutaneous wound healing in a way which indicates that PPARα is implicated preferentially during the early stages of the process, and PPARβ during the

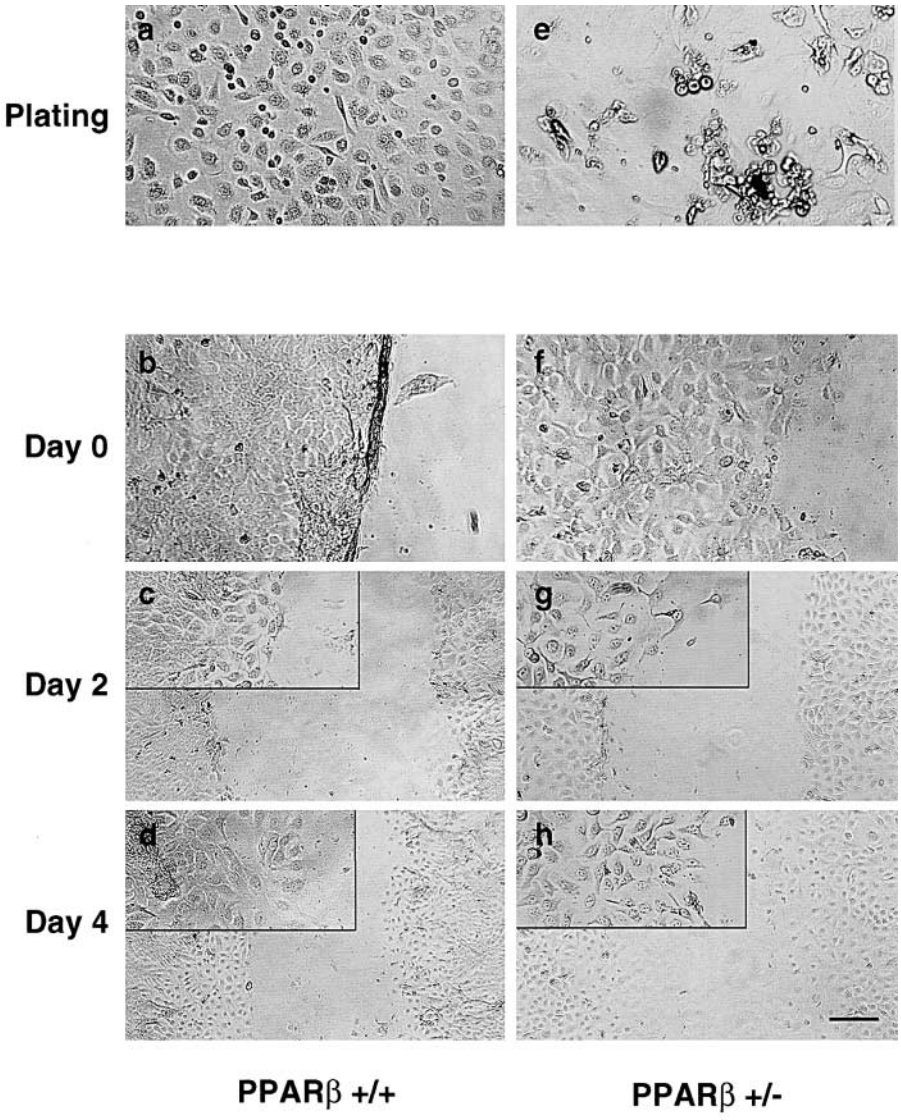

Figure 9. **PPARβ+/− primary keratinocytes show impaired adhesion and migration properties.** Primary keratinocytes isolated from skin of PPARβ+/+ (a–d) or PPARβ+/− (e–h) newborn pups. (a) Wild-type keratinocytes 24 h after plating; (e) PPARβ+/− keratinocytes 3 d after plating. (b–d and f–h) Wounded cultures of primary keratinocytes: scrape wounds were made at day 0 (day 0 corresponds to the obtention of 70–80% confluent cell culture) (b and f). Panels c and g and d and h represent the wounds at day 2 and 4 after scraping, respectively. Bar: (a, b, e, f, and insets) 100 μm; (c, d, g, and h) 200 μm.

whole healing period, which correlates with their reactivated expression pattern after skin biopsy. Moreover, the results indicate that the recruitment of immune cells is impaired during the early inflammatory phase in the PPARα−/− mice, whereas the delay observed in PPARβ mutant mice is likely to be due to impaired adhesion and migration capacities of the keratinocytes.

Discussion

This work was aimed at characterizing the expression and function of the three PPAR isotypes in the fetal and adult skin. In short, we have demonstrated that the developing skin expresses the three PPAR isotypes with specific spatiotemporal patterns. In the unchallenged adult interfollicular epidermis, the three PPAR isotypes are undetectable, whereas PPARα and PPARβ are upregulated upon diverse insults that result in both inflammation and cell proliferation. The use of mutant mice for each of the PPAR isotypes helped in deciphering their specific role in vivo. Although PPARγ+/− mice do not present any phenotype, PPARα null mice have a transient and initial delay in wound healing and PPARβ+/− mice exhibit a delay during the whole healing process, postponing its completion by 2–3 d.

Differential expression of PPARs in the developing epidermis and during postnatal stages

Here we show that the three PPAR isotypes are expressed during embryonic epidermal development, starting before stratification and differentiation of the epidermis, and in early postnatal stage, whereas they are below detection levels in the adult interfollicular epidermis. PPARα and β were also found to be present at low levels in the fetal dermis. This distribution strongly suggests that PPARs are not required, or only at very low levels, for normal skin homeostasis in the adult, but participate in the fetal maturation and differentiation of the skin. The reexpression of PPARs during wound healing, with a similar overall pattern as seen during development, provides a valuable experimental model. Indeed, it implies that wound healing reactivates processes that are normally part of the developmental program rather than those involved in normal adult skin renewal.

Development of a functional barrier during late embryonic development (Hardman et al., 1998) correlates with both changes in the organization and the abundance of the extracellular lipid lamellar structures (Aszterbaum et al., 1992; Hardman et al., 1998). This is in part reflected with fetal keratohyalin granules, which contain large lipid-like droplets (DuBrul, 1972). In the adult, the epidermis is continuously renewed through proliferation of the cells forming the basal layer, and the daughter cells differentiate along migration to the upper cornified layer. No large lipid-like droplets are seen, suggesting a difference in the lipid content and organization with respect to the fetal skin. However, at the molecular level the difference in the mechanisms involved in the fetal and adult epidermis are poorly understood. Thus, the different PPAR expression patterns might be of high interest with respect to the molecular events underlying the differences between fetal and adult epidermis.

Genetic analysis of specific roles of PPARα, β, and γ in skin maturation

PPAR activators accelerate rat epidermal development (Hanley et al., 1997b) and can increase the level of expression of several keratinocyte terminal differentiation markers in rat keratinocyte culture (Hanley et al., 1998). However, under normal conditions, no altered skin phenotype has been detected so far in PPARα null mice (Lee et al., 1995). Similarly, no skin alteration was reported for the PPARγ null mouse, born after placental rescue using tetraploid cells (Barak et al., 1999), and PPARγ+/− mice appear normal as well (herein and Kubota et al. [1999]). Finally, as mentioned above, the PPARβ null mice that we and others (Peters et al., 2000) have obtained exhibit no obvious skin defect, and the PPARβ+/− mice appear normal as well. At this point, it is of interest to note that most of the previous mutant mouse lines, resulting from targeted disruption of nuclear hormone receptors genes, failed to exhibit a skin phenotype even though there is evidence for a role of these nuclear hormone receptors in the skin. The absence of a skin phenotype at birth in the various PPAR mutant mice might be due to a functional redundancy of the three isotypes. Alternatively, as with many processes during development, gene expression in skin formation may depend on a regulatory network rather than on a linear cascade, allowing for adaptation to take place during in utero development. In adult skin, the absence or below in situ hybridization detection level of PPAR expression in interfollicular epidermis is consistent with the absence of an altered skin in the mutant mice. However, a careful histological observation and Ki67 quantification indicated a small but reproducible amount of proliferative cells in PPARβ+/− mice, suggesting that even in unchallenged condition, skin homeostasis is slightly altered in the PPARβ+/− mice.

PPARα and the inflammation stage in wound healing

Skin wound healing can be divided into three major overlapping and interacting phases which follow a defined time sequence: inflammation, new tissue formation, including the differentiation of a neoepithelium, and remodeling (Fig. 7). The initial inflammatory phase after an injury is a beneficial step that precedes normal repair of the wound. It allows clot formation and control of infectious agents, favors vascularization, and allows local afflux of growth factors. Attracted by chemotactic factors and chemokines, neutrophils accumulate first in the wound bed and serve as an initial line of defense and source of proinflammatory cytokines. After neutrophils, monocytes/macrophages are recruited and, in addition to providing an immune response, release large amounts of growth factors and cytokines. If not controlled, inflammation can contribute to pathological healing, such as extensive scarring or fibrosis, which underscore the importance of a tight control of this early phase of the healing process. The pattern of PPARα expression, mainly in the very first days after the injury nicely overlaps the timing of the inflammation stage. Accordingly, PPARα null mice exhibit a transient but significant delay in the healing process in the early phase. Since we showed that PPARα null mice exhibit normal keratinocyte proliferation after TPA treatment of the dorsal epidermis, the delay in the skin healing process of the PPARα null mice is unlikely to be due to an uncontrolled proliferation. Moreover, the quantification of the inflammatory infiltration shows that the recruitment of the neutrophils and monocytes/macrophages to the wound bed are both impaired in the PPARα−/− mice during the very early inflammatory phase. This strongly suggests that the transient delay of healing observed in the PPARα null mice is due to uncontrolled inflammation at the wound site. The normal recruitment of immune cells is then restored in the PPARα−/− mice, which reflects the ability of these mice to finally reestablish appropriate inflammation control and, consequently, normal resolution of the healing process. These data correlate with previous observations that PPARα participates in the control of an inflammatory response (Devchand et al., 1996; Staels et al., 1998). At the molecular level, specific quantification of chemotactic factors and chemokines released in the wound bed will help in deciphering the mechanism, leading to altered recruitment of immune cells in the PPARα null mice. Of particular interest will be the measurement of the levels of IL-1α released at the wound site. Indeed, several reports indicate that keratinocytes, after a skin injury, may participate in the early inflammatory phase by secreting large amounts of preformed active IL-1α (Kupper, 1990; Kupper and Groves, 1995). In this context, it is certainly noteworthy that our results demonstrate that PPARα expression is upregulated in the keratinocytes at the wound edges during the inflammatory phase of skin wound healing.

In contrast, PPARγ seems not to be involved in skin inflammation as it is not expressed in any of the models tested in our study.

PPARβ expression and keratinocyte proliferation, adhesion, and migration

In the second step of wound healing, which begins within hours of a skin injury, the keratinocytes will start to migrate from the wound edges and proliferate to cover the wound. The final stage then consists of stratification and differentiation of the neoepidermis and colonization of the epithelium by the nonkeratinocyte cells (e.g., immune cells). Upregulation of PPARβ in the keratinocytes takes place during all these successive processes. In addition, the reexpression of PPARβ in two models of intense keratinocyte prolifera-

tion (TPA and hair plucking) strengthens the link between PPARβ and the control of cell proliferation. A role of PPARβ in the control of epithelial cell proliferation has also been recently described in colon cancer cells (He et al., 1999), whereas Matsuura et al. (1999) associated an increased PPARβ expression to induced human keratinocyte differentiation in vitro and in vivo. Interestingly, our PPARβ mutant mice exhibit an altered control of keratinocyte proliferation, characterized by a hyperproliferative reaction, in response to TPA stimulation and hair plucking. No defect is observed in PPARβ+/− keratinocyte–terminal differentiation, as suggested by the expression of keratinocyte differentiation markers. Consistent with these observations, an enhanced hyperplastic response, associated to a higher expression of cell cycle proteins but normal expression of differentiation markers, was reported recently in the epidermis of PPARβ null mice (Peters et al., 2000). In addition to this observation, and very importantly, we also report a defect in PPARβ mutant keratinocyte adhesion and migration capacities, as observed in primary keratinocyte cultures. This result strongly suggests that a keratinocyte migration defect is at least partially responsible for the delay in the healing process in the PPARβ+/− mice. In the whole animal, indeed, quantification of the cells at the edges of a wound indicates that the keratinocytes are slightly more numerous in the PPARβ mutant wounds, consistent with an increased proliferation and slower migration of these cells. Thus, although we cannot rule out a more general implication of PPARβ in the skin, our data, together with the recently reported phenotype of the PPARβ null mice, provide evidence for the necessity of an increased PPARβ expression to control a well balanced proliferation/differentiation process and efficient keratinocyte migration required for nonpathological wound healing.

In conclusion, our observations reveal an important role of PPARα and PPARβ in epidermis repair. In addition and very importantly, despite sharing many characteristics these two isotypes clearly do not have redundant functions. Their respective expression and function are complementary and cover the different phases of skin wound–healing processes. Thus, elucidation of the molecular mechanisms responsible for the differential expression of PPARα in the various inflammation models, as well as those leading to PPARβ activation in the proliferating stage and cessation of its activity upon completion of healing, should be very informative with respect to the potential use of PPARα and PPARβ agonists, or antagonists when available, as therapeutic tools in skin affections.

Materials and methods

Tissue preparation and sections

Skin samples were embedded in tissue-freezing medium (Leica). 8-μm cryostat tissue sections were mounted on slides and postfixed in 4% paraformaldehyde-PBS (10 min, 4°C). After washings in PBS, sections were used either for histological staining (hematoxilin-eosin, Van Gieson [collagen]) or resorcin/fuchsine [elastin]) immunofluorescent labeling, or in situ hybridization.

In situ hybridization

Mouse PPARα–, β–, and γ–specific sense (S) and antisense (AS) digoxygenin–labeled riboprobes were obtained by in vitro transcription, using mouse PPAR α, β, or γ A/B domain cDNA as a template (size of the probes: PPARα AS, 230 b; PPARα S, 230 b; PPARβ AS, 200 b; PPARβ S, 170 b; PPARγ AS, 230 b; PPARγ S, 222 b). The digoxygenin incorporation and the specificity of the probes were tested on slot-blot hybridizations. In situ hybridization was processed as described previously (Braissant et al., 1996).

Immunofluorescence

The keratin 6, 10, and 14 cytoskeletal protein (BabCo), loricrin (BabCo), involucrin (BabCo), and the Ki67 nuclear antigen (Novo Castra) were detected using rabbit polyclonal primary antibodies. For the Ki67 labeling, an antigen-unmasking step was performed (citrate buffer, pH 6, 100°C, 10 mn). The slides were then processed as followed: 1 × PBS, 0.1% BSA/30 mn/RT; primary antibodies in 1 × PBS buffer, 0.1% BSA/2 h/RT; washings in 1 × PBS buffer; FITC-conjugated goat anti–rabbit IgG secondary antibody (Sigma-Aldrich) in 1 × PBS buffer, 0.1% BSA/1 h/RT. The slides were subsequently washed and mounted before microscopic observation.

RNase protection assays

Mouse PPARα–, β– and γ–specific antisense riboprobes were obtained by in vitro transcription with the T7 or SP6 RNA polymerase, using mouse PPARα (A/B domain), β or γ (A/B/C domain) cDNA subcloned in the pGEM3Zf(+) (Promega) as templates. The 228-bases PPARα probe, the 272-bases PPARβ probe, and the 331-bases PPARγ probe resulted in digested fragments of 192, 254, and 295 bp, for PPARα, PPARβ, and PPARγ, respectively. The L27 probe has been described previously (Lemberger et al., 1994). For all PPAR probes, a ratio of 1:1 of α^{32}-P–UTP to cold UTP was used, whereas a 1:20 ratio of L27 probe was used. Incorporation and specific activity of each probe was determined after purification via Rneasy Clean-Up (QIAGEN).

Direct lysate RPA was carried out as described by the manufacturer (Ambion) with some modifications. In brief, tissues were lysed in Lysis/Denaturation solution (2 mg/ml) and clarified by centrifugation (Qiashredder; QIAGEN). 20 μL of lysate was hybridized to 1 ng of specific PPAR probes (10^9 cpm/μg) and 10 ng of L27 probe (10^8 cpm/μg). RNase digestion (10 U/ml RNaseA; 400 U/ml RNaseT1) was carried out for all probes at 37°C/20 min. The products of RPA were resolved in a 6% electrolyte-gradient denaturing polyacrylamide gel. Gels were dried and exposed on phosphor screen of a StormImager 840 (Molecular Dynamics). Quantitative analysis was performed by using IQuant 2.5 software. PPAR mRNA expression was normalized to the previously calculated specific activity of the probe and to L27 mRNA expression. The PPAR/L27 ratio was further normalized to the UTP content of each PPAR probe.

Wound-healing experiments

The hair follicle cycle of each mouse was synchronized by shaving the back of the animal 2 wk before starting the experiment. Control and transgenic mice were then anesthetized, shaved, and a full thickness middorsal wound (0.5-cm^2 surface, square shaped) was created by excising the skin and the underlying *panniculus carnosus*. The wounds were then allowed to dry and form a scab. Wound closure was measured daily in a double-blinded fashion, on young (6–8 wk) and old (12–18 mo) animals until complete healing of both control and transgenic mice. The surfaces of the wounds were measured by a single individual by covering each wound with a transparent plastic sheet and tracing the wound area on anesthetized animals (Gross et al., 1995; Streit et al., 2000). Wound areas were quantified (Sigma-Scan; Sigma-Aldrich) and were standardized and expressed as a percentage of the initial wound size (100%). The mean values (n = 8–10 animals) were plotted for each time point, ± SEM. A Student's t test was used for comparison of the control and PPAR mutant groups.

To examine PPAR expression at the site of the injury, the mouse was sacrificed and an area including the scab and the complete epithelial edges of the wounds was excised at each time point. For each mouse, a control of normal dorsal skin was taken at distance from the wounded tissue.

Inflammatory infiltration

Neutrophil and monocyte/macrophage infiltration was quantified on tissue sections of PPARα+/+ and −/− mice. Sections from wounds at day 1, 3, and 5 postwounding were hematoxilin/eosin stained. The density of neutrophils and monocytes/macrophages was determined by manually counting the infiltrating immune cells based on morphological criteria in five standardized microscopic fields (400× magnification) for each wound. Statistical analysis of the data is based on the Student's t test.

Keratinocyte proliferation assays

TPA application. 5 nmoles of TPA in 200 μl ethanol was topically applied on the shaved left part of the dorsal epidermis of control and transgenic animals. As a control, the right part of the dorsal epidermis, away from the TPA-treated part, was treated with vehicle only. Samples were harvested 2 d after the TPA application.

Hair plucking. For synchronization purposes, hair was plucked a first time on a 0.5-cm^2 dorsal surface of control and transgenic mice. After a period of 10 d, the same surface was plucked a second time and the treated region was dissected 2 d later. As a control, skin samples were taken at a distance from the plucked surface.

The dissected tissues were then processed as described above and used for histological staining, immunolabeling, or in situ hybridization. Quantitative analysis of the mean epidermal thickening and the Ki67-positive cells was performed using the Object Image software.

Primary keratinocyte culture and in vitro scraping wound

Mouse keratinocytes were isolated from epidermis as reported by Hager et al. (1999) with the following modifications: the epidermis was separated from the dermis after overnight incubation at 4°C in 2.5 U/ml of Dispase. The epidermis was placed in a 50-ml centrifuge tube with 10 ml of keratinocyte serum–free medium and the tube was given 50 firm shakes. Keratinocytes were resuspended in keratinocyte serum–free medium containing 0.05 mM Ca^{2+} and 0.1 ng/ml epidermal growth factor, and seeded at 2×10^5 cells/cm^2 for the wild-type keratinocytes, and at $4–6 \times 10^5$ cells/cm^2 for the mutant keratinocytes. Keratinocytes were used after 2–3 passages.

For the scraping experiment, keratinocytes were cultured in a 60-mm diameter tissue culture dish. At 70–80% confluency, a scrape (~1.5–2 mm) was made (day 0) across the diameter using a cell scraper. At the indicated time, pictures of the cells near the edges were taken until complete closure of the scrape wound. In total, the cells were maintained in culture for 2–3 wk, depending on their genotype.

We thank Nathalie Deriaz, Mai Perroud, Tatiana Favez, Antoine Genoz, Marianne Friedli, Takeshi Imai, Andrée Dierich, and Marianne LeMeur for excellent assistance. We are grateful to Gary McMaster, Pascal Neuville, and Julio Gabbiani for useful discussions, to François Conquet for the gift of the 129/SV mouse ES cells genomic library, and to Charles Weissmann for the gift of the TK-NEO-UMS vector.

This work was supported by the Swiss National Science Foundation (grants to Walter Wahli and to Béatrice Desvergne), by the Etat de Vaud, by the Human Frontier Science Program Organization, and by Parke-Davis Pharmaceutical Research.

Submitted: 29 November 2000
Accepted: 16 July 2001

References

Aszterbaum, M., G.K. Menon, K.R. Feingold, and M.L. Williams. 1992. Ontogeny of the epidermal barrier to water loss in the rat: correlation of function with stratum corneum structure and lipid content. *Pediatr. Res*. 31:308–317.

Aszterbaum, M., K.R. Feingold, G.K. Menon, and M.L. Williams. 1993. Glucocorticoids accelerate fetal maturation of the epidermal permeability barrier in the rat. *J. Clin. Invest*. 91:2703–2708.

Barak, Y., M.C. Nelson, E.S. Ong, Y.Z. Jones, P. Ruiz-Lozano, K.R. Chien, A. Koder, and R.M. Evans. 1999. PPAR γ is required for placental, cardiac, and adipose tissue development. *Mol. Cell*. 4:585–595.

Bickenbach, J.R., J.M. Greer, D.S. Bundman, J.A. Rothnagel, and D.R. Roop. 1995. Loricrin expression is coordinated with other epidermal proteins and the appearance of lipid lamellar granules in development. *J. Invest. Dermatol*. 104:405–410.

Braissant, O., and W. Wahli. 1998. Differential expression of peroxisome proliferator-activated receptor-α, -β, and -γ during rat embryonic development. *Endocrinology*. 139:2748–2754.

Braissant, O., F. Foufelle, C. Scotto, M. Dauca, and W. Wahli. 1996. Differential expression of peroxisome proliferator-activated receptors (PPARs): tissue distribution of PPAR-α, -β, and -γ in the adult rat. *Endocrinology*. 137:354–366.

Crowe, M.J., T. Doetschman, and D.G. Greenhalgh. 2000. Delayed wound healing in immunodeficient TGF-β 1 knockout mice. *J. Invest. Dermatol*. 115:3–11.

Desvergne, B., and W. Wahli. 1999. Peroxisome proliferator-activated receptors: Nuclear control of metabolism. *Endocr. Rev*. 20:649–688.

Devchand, P.R., H. Keller, J.M. Peters, M. Vazquez, F.J. Gonzalez, and W. Wahli. 1996. The PPARα-leukotriene B4 pathway to inflammation control. *Nature*. 384:39–43.

Downing, D.T. 1992. Lipid and protein structures in the permeability barrier of mammalian epidermis. *J. Lipid Res*. 33:301–313.

DuBrul, E.F. 1972. Fine structure of epidermal differentiation in the mouse. *J. Exp. Zool*. 181:145–158.

Echtermeyer, F., M. Streit, S. Wilcox-Adelman, S. Saoncella, F. Denhez, M. Detmar, and P. Goetinck. 2001. Delayed wound repair and impaired angiogenesis in mice lacking syndecan- 4. *J. Clin. Invest*. 107:R9–R14.

Elias, P.M. 1983. Epidermal lipids, barrier function, and desquamation. *J. Invest. Dermatol*. 80:44s–49s.

Elias, P.M., and G.K. Menon. 1991. Structural and lipid biochemical correlates of the epidermal permeability barrier. *Adv. Lipid Res*. 24:1–26.

Gallucci, R.M., P.P. Simeonova, J.M. Matheson, C. Kommineni, J.L. Guriel, T. Sugawara, and M.I. Luster. 2000. Impaired cutaneous wound healing in interleukin-6-deficient and immunosuppressed mice. *FASEB J*. 14:2525–2531.

Gross, J., W. Farinelli, P. Sadow, R. Anderson, and R. Bruns. 1995. On the mechanism of skin wound "contraction": a granulation tissue "knockout" with a normal phenotype. *Proc. Natl. Acad. Sci. USA*. 92:5982–5986.

Hager, B., J.R. Bickenbach, and P. Fleckman. 1999. Long-term culture of murine epidermal keratinocytes. *J. Invest Dermatol*. 112:971–976.

Hanley, K., U. Rassner, P.M. Elias, M.L. Williams, and K.R. Feingold. 1996a. Epidermal barrier ontogenesis: maturation in serum-free media and acceleration by glucocorticoids and thyroid hormone but not selected growth factors. *J. Invest. Dermatol*. 106:404–411.

Hanley, K., U. Rassner, Y. Jiang, D. Vansomphone, D. Crumrine, L. Komuves, P.M. Elias, K.R. Feingold, and M.L. Williams. 1996b. Hormonal basis for the gender difference in epidermal barrier formation in the fetal rat. Acceleration by estrogen and delay by testosterone. *J. Clin. Invest*. 97:2576–2584.

Hanley, K., U.P. Devaskar, S.J. Hicks, Y. Jiang, D. Crumrine, P.M. Elias, M.L. Williams, and K.R. Feingold. 1997a. Hypothyroidism delays fetal stratum corneum development in mice. *Pediatr. Res*. 42:610–614.

Hanley, K., Y. Jiang, D. Crumrine, N.M. Bass, R. Appel, P.M. Elias, M.L. Williams, and K.R. Feingold. 1997b. Activators of the nuclear hormone receptors PPARα and FXR accelerate the development of the fetal epidermal permeability barrier. *J. Clin. Invest*. 100:705–712.

Hanley, K., Y. Jiang, S.S. He, M. Friedman, P.M. Elias, D.D. Bikle, M.L. Williams, and K.R. Feingold. 1998. Keratinocyte differentiation is stimulated by activators of the nuclear hormone receptor PPARα. *J. Invest. Dermatol*. 110:368–375.

Hanley, K., L.G. Komuves, D.C. Ng, K. Schoonjans, S.S. He, P. Lau, D.D. Bikle, M.L. Williams, P.M. Elias, J. Auwerx, and K.R. Feingold. 2000. Farnesol stimulates differentiation in epidermal keratinocytes via PPARα. *J. Biol. Chem*. 275:11484–11491.

Hardman, M.J., P. Sisi, D.N. Banbury, and C. Byrne. 1998. Patterned acquisition of skin barrier function during development. *Development*. 125:1541–1552.

He, T.C., T.A. Chan, B. Vogelstein, and K.W. Kinzler. 1999. PPARΔ is an APC-regulated target of nonsteroidal anti-inflammatory drugs. *Cell*. 99:335–345.

Imakado, S., J.R. Bickenbach, D.S. Bundman, J.A. Rothnagel, P.S. Attar, X.J. Wang, V.R. Walczak, S. Wisniewski, J. Pote, J.S. Gordon, et al. 1995. Targeting expression of a dominant-negative retinoic acid receptor mutant in the epidermis of transgenic mice results in loss of barrier function. *Genes Dev*. 9:317–329.

Kaya, G., I. Rodriguez, J.L. Jorcano, P. Vassalli, and I. Stamenkovic. 1997. Selective suppression of CD44 in keratinocytes of mice bearing an antisense CD44 transgene driven by a tissue-specific promoter disrupts hyaluronate metabolism in the skin and impairs keratinocyte proliferation. *Genes Dev*. 11:996–1007.

Kubota, N., Y. Terauchi, H. Miki, H. Tamemoto, T. Yamauchi, K. Komeda, S. Satoh, R. Nakano, C. Ishii, T. Sugiyama, et al. 1999. PPAR γ mediates high-fat diet-induced adipocyte hypertrophy and insulin resistance. *Mol. Cell*. 4:597–609.

Kupper, T.S. 1990. Immune and inflammatory processes in cutaneous tissues. Mechanisms and speculations. *J. Clin. Invest*. 86:1783–1789 (erratum published 87:753).

Kupper, T.S., and R.W. Groves. 1995. The interleukin-1 axis and cutaneous inflammation. *J. Invest. Dermatol*. 105:62S–66S.

Lee, S.S., T. Pineau, J. Drago, E.J. Lee, J.W. Owens, D.L. Kroetz, S.P. Fernandez, H. Westphal, and F.J. Gonzalez. 1995. Targeted disruption of the α isoform of the peroxisome proliferator-activated receptor gene in mice results in abolishment of the pleiotropic effects of peroxisome proliferators. *Mol. Cell. Biol*. 15:3012–3022.

Lemberger, T., B. Staels, R. Saladin, B. Desvergne, J. Auwerx, and W. Wahli. 1994. Regulation of the peroxisome proliferator-activated receptor α gene by glucocorticoids. *J. Biol. Chem*. 269:24527–24530.

Li, M., A.K. Indra, X. Warot, J. Brocard, N. Messaddeq, S. Kato, D. Metzger, and P. Chambon. 2000. Skin abnormalities generated by temporally controlled RXRα mutations in mouse epidermis. *Nature*. 407:633–636.

Li, M., H. Chiba, X. Warot, N. Messaddeq, C. Gerard, P. Chambon, and D.

Metzger. 2001. RXRα ablation in skin keratinocytes results in alopecia and epidermal alterations. *Development*. 128:675–688.

Matsuura, H., H. Adachi, R.C. Smart, X. Xu, J. Arata, and A.M. Jetten. 1999. Correlation between expression of peroxisome proliferator-activated receptor β and squamous differentiation in epidermal and tracheobronchial epithelial cells. *Mol. Cell. Endocrinol*. 147:85–92.

Navarro, J.M., J. Casatorres, and J.L. Jorcano. 1995. Elements controlling the expression and induction of the skin hyperproliferation-associated keratin K6. *J. Biol. Chem*. 270:21362–21367.

Nuclear Receptor Nomenclature Committee. 1999. A unified nomenclature system for the nuclear receptor superfamily (letter). *Cell*. 97:161–163.

Peters, J.M., S.S. Lee, W. Li, J.M. Ward, O. Gavrilova, C. Everett, M.L. Reitman, L.D. Hudson, and F.J. Gonzalez. 2000. Growth, adipose, brain, and skin alterations resulting from targeted disruption of the mouse peroxisome proliferator-activated receptor β. *Mol. Cell Biol*. 20:5119–5128.

Rivier, M., I. Safonova, P. Lebrun, C.E. Griffiths, G. Ailhaud, and S. Michel. 1998. Differential expression of peroxisome proliferator-activated receptor subtypes during the differentiation of human keratinocytes. *J. Invest Dermatol*. 111:1116–1121.

Roop, D. 1995. Defects in the barrier. *Science*. 267:474–475.

Saitou, M., S. Sugai, T. Tanaka, K. Shimouchi, E. Fuchs, S. Narumiya, and A. Kakizuka. 1995. Inhibition of skin development by targeted expression of a dominant-negative retinoic acid receptor. *Nature*. 374:159–162.

Schurer, N.Y., and P.M. Elias. 1991. The biochemistry and function of stratum corneum lipids. *Adv. Lipid Res*. 24:27–56.

Staels, B., W. Koenig, A. Habib, R. Merval, M. Lebret, I.P. Torra, P. Delerive, A. Fadel, G. Chinetti, et al. 1998. Activation of human aortic smooth-muscle cells is inhibited by PPARα but not by PPARγ activators. *Nature*. 393:790–793.

Streit, M., P. Velasco, L. Riccardi, L. Spencer, L.F. Brown, L. Janes, B. Lange-Asschenfeldt, K. Yano, T. Hawighorst, L. Iruela-Arispe, and M. Detmar. 2000. Thrombospondin-1 suppresses wound healing and granulation tissue formation in the skin of transgenic mice. *EMBO J*. 19:3272–3282.

Westergaard, M., J. Henningsen, M.L. Svendsen, C. Johansen, U.B. Jensen, H.D. Schroder, I. Kratchmarova, R.K. Berge, L. Iversen, L. Bolund, K. Kragballe, and K. Kristiansen. 2001. Modulation of keratinocyte gene expression and differentiation by PPAR-selective ligands and tetradecylthioacetic acid. *J. Invest. Dermatol*. 116:702–712.

Woodley, D.T. 1996. Reepithelialization. *In* The Molecular and Cellular Biology of Wound Repair. R.A.F. Clark, editor. Plenum Press, New York. 339–354.